ELSEVIER

Journal of Alloys and Compounds 317–318 (2001) 573–577

Journal of ALLOYS AND COMPOUNDS

www.elsevier.com/locate/jallcom

# The high temperature oxidation of a two-phase Ag–Y alloy under 1 and $10^{-20}$ atm $O_2$

Y. Niu[a,b], F. Gesmundo[b,*], M. Al-Omary[c], J. Song[a]

[a]*State Key Laboratory for Corrosion and Protection, Institute of Metals Research, 110015 Shenyang, China*
[b]*Dipartimento di Ingegneria Chimica, Università di Genova, Fiera del Mare, Pad. D, 16129 Genova, Italy*
[c]*Dipartiment of Basic Sciences, University of Sharjah, P.O. Box 28267 Sharjah, United Arab Emirates*

**Abstract**

A silver-based alloy containing about 8 wt% Y (Ag–8Y) has been oxidized under 1 atm and $10^{-20}$ atm $O_2$ at 700°C. The alloy contains a mixture of a solid solution of Y in Ag (α phase) with an eutectic mixture of the α phase with the intermetallic compound $Ag_{51}Y_{14}$ (β phase). The oxidation rate in 1 atm $O_2$ is very fast and follows the parabolic rate law to a good approximation. Oxidation under low $P(O_2)$ is much slower and quite irregular with large deviations from an average parabolic behavior. Under 1 atm $O_2$ the alloy undergoes only an internal oxidation of Y without any significant outward Y diffusion, as a result of a fast oxygen penetration. Under low $P(O_2)$ the alloy forms an almost continuous $Y_2O_3$ layer containing Ag particles, plus a region of internal oxidation of Y much thinner than in 1 atm $O_2$. In both cases the alloy forms also an external layer of pure Ag metal, more continuous for the oxidation under 1 atm $O_2$. The $Y_2O_3$ particles within the alloy change shape with depth, being small and globular close to the alloy surface but larger and acicular, elongated nearly perpendicularly to the alloy surface, at larger depths. For samples oxidized under $10^{-20}$ atm $O_2$ the volume fraction of internal oxide increases with depth in the alloy, tending to form an almost continuous oxide layer close to the front of internal oxidation, except over regions very rich in Ag. 

*Keywords:* Y; Ag; Two-phase alloys; Oxidation

## 1. Introduction

Yttrium is one of the reactive elements, frequently added at very small concentrations to alloys for use at high temperatures forming protective chromia or alumina scales to reduce their oxidation rate and minimize scale spalling [1,2]. Ag and Y have a very small mutual solubility and form three intermetallic compounds with very restricted stability fields [3]. Thus, in almost all their composition range Ag–Y alloys are two-phase: in addition, Ag is noble with respect to oxygen, while the Y oxide is very stable [4]. The oxidation of binary two-phase alloys presents a number of new aspects with respect to the much better known behavior of binary solid-solution alloys [5–8]. The scaling of an Y-dilute Ag–Y alloy at 700°C has been examined under two different oxygen pressures to study the effect of this parameter on the kinetics and mechanism of oxidation as well as on the microstructure of the corroded samples.

## 2. Experimental details

An Ag–Y alloy with a nominal Y content of 8 wt% (Ag–8Y) has been prepared by arc-melting an appropriate mixture of the two pure metals under a Ti-gettered inert atmosphere. In agreement with the Ag–Y phase diagram [3], the alloy (Fig. 1) contains a continuous network of proeutectic solid solution of Y in Ag (α phase, light), mixed with darker islands composed of an eutectic mixture of the α phase with the intermetallic compound $Ag_{51}Y_{14}$ (β phase, dark). Alloy samples were cut from the original ingot, abraded down to 600 grit emery paper, washed and dried immediately before use. Oxidation tests were carried out both in 1 atm of pure oxygen and using an $H_2$–$CO_2$ mixture containing 79.35 vol% $CO_2$, which under equilibrium condition at 700°C provides an oxygen pressure of $10^{-20}$ atm. The scaling kinetics were measured using a

*Corresponding author. Tel.: +39-010-353-6040; fax: +39-010-353-6028.

*E-mail address:* gesmundo@unige.it (F. Gesmundo).

0925-8388/01/$ – see front matter 
PII: S0925-8388(00)01390-6

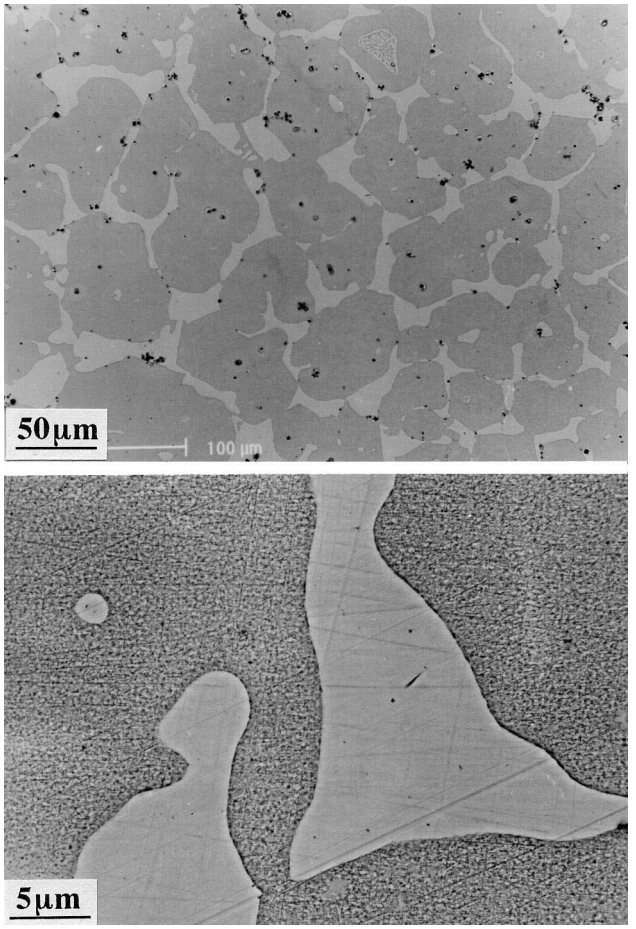


Fig. 1. Microstructure of Ag–8Y (SEM/BEI). Light phase = α (ss of Y in Ag); dark islands = mixtures of α + $Ag_{51}Y_{14}$ (β phase).

Cahn microbalance mod. 2000. Corroded samples were examined by Scanning Electron Microscopy (SEM) and Energy-Dispersive X-Ray Microanalysis (EDX) to examine the distribution and composition of phases.

## 3. Results

The weight gain curves for the oxidation of Ag–8Y at 700°C are shown in Fig. 2. Oxidation in 1 atm $O_2$ is quite fast and follows the parabolic rate law to a good approximation, with a rate constant $k_p = 1.37 \times 10^{-9}$ $g^2$ $cm^{-4}$ $s^{-1}$ up to 2 h oxidation: longer times were not examined due to the fast scaling. Oxidation under $10^{-20}$ atm $O_2$ is much slower and quite irregular, showing large deviations from a parabolic behavior, with an average rate constant of $2.7 \times 10^{-11}$ $g^2$ $cm^{-4}$ $s^{-1}$ after a short initial faster stage.

Oxidation of Ag–8Y in 1 atm $O_2$ produces only an internal oxidation (io) of Y within a matrix of pure Ag, which after 2 h is about 80 μm thick (Fig. 3). Externally to the alloy, an Ag layer about 3 μm thick is also present. The microstructure of the internal oxidation zone (ioz) follows closely that of the original alloy, since the α phase

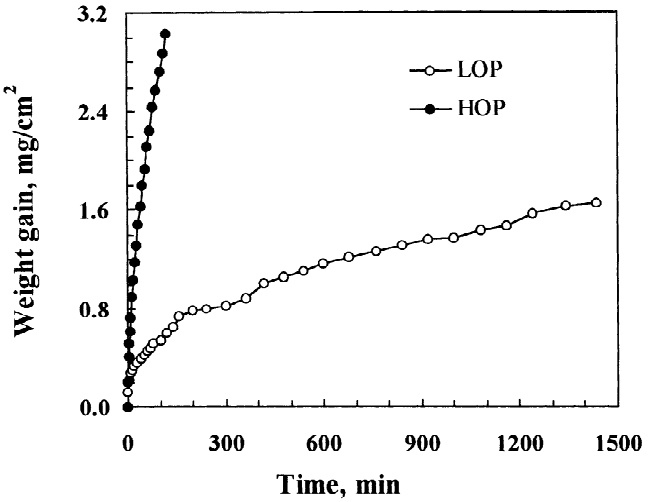


Fig. 2. Kinetics of oxidation of Ag–8Y at 700°C under 1 (HOP) and $10^{-20}$ (LOP) atm $O_2$.

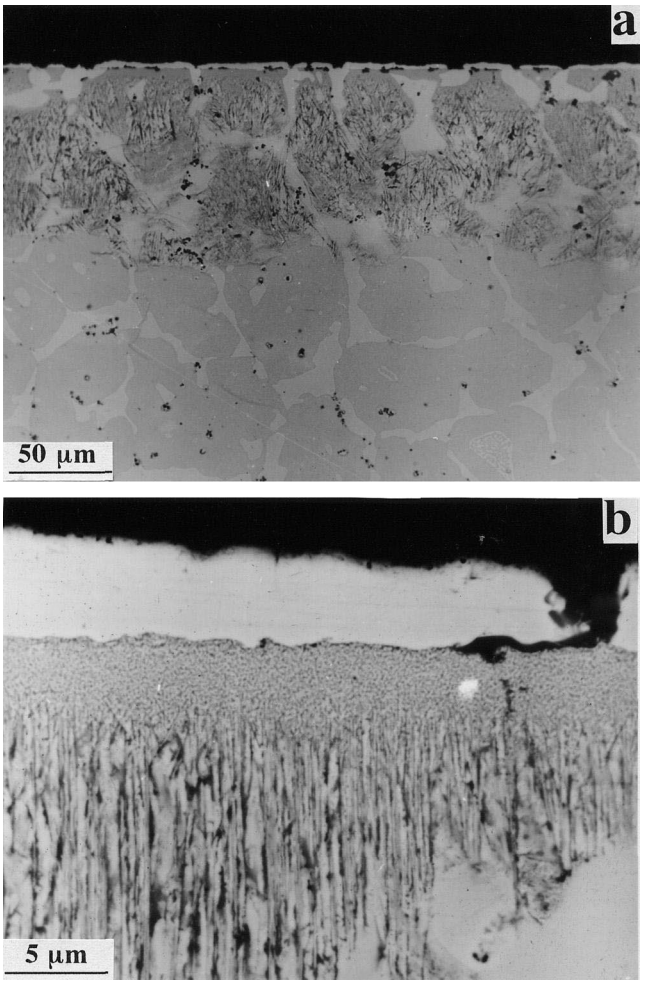


Fig. 3. Micrographs (SEM/BEI) of a cross section of Ag–8Y oxidized at 700°C under 1 atm $O_2$ for 2 h. (a) General view; (b) Enlarged view of the outer scale region.

regions are almost free from $Y_2O_3$, while their number, size and spatial distribution are the same as those of the corresponding islands in the original alloy. On the contrary, the alloy regions containing the $\alpha+\beta$ eutectic mixture are converted into a mixture of Ag and $Y_2O_3$. Moreover, the morphology of the internal oxide particles changes with depth in the alloy. In fact, close to the alloy surface (down to about 6 μm) the oxide particles are small and globular, while deeper into the alloy they become acicular and are preferentially elongated perpendicularly to the alloy surface, similar to the rods observed in the io of Ni–Al alloys [9]. Moreover, no significant Y depletion develops in the alloy behind the internal oxidation front (iof), as evidenced by its normal two-phase structure.

Oxidation of Ag–8Y under low $P(O_2)$ at 700°C produces complex scales, as shown in Fig. 4. The outermost region, composed of irregular Ag nodules scattered over the sample surface, is followed by a dark $Y_2O_3$ layer containing Ag particles forming a thin discontinuous layer. Beneath this oxide layer there is again an ioz of Y. As for the oxidation in 1 atm $O_2$, the oxide particles are quite small and globular close to the gas, but become elongated and acicular after a critical depth. Finally, close to the iof the internal oxide has a larger volume fraction and tends to form a continuous layer. Actually, these regions contain also significant amounts of Ag (about 75 at%, neglecting oxygen) and therefore are much lighter than the external pure $Y_2O_3$ layer. Moreover, behind the iof there is an Y-depleted zone, where the β phase has disappeared from the $\alpha+\beta$ eutectic mixture, leaving a continuous α phase layer.

Contrary to the results for the oxidation in 1 atm $O_2$, the microstructure of the ioz under low P ($O_2$) is not related to that of the original alloy. In fact, the β phase dissolves before the arrival of oxygen to provide Y to the ioz, so that the original alloy microstructure is destroyed. The depth of this region is of only about 20 μm after 24 h oxidation, and thus is much smaller than what measured after only 2 h of exposure to 1 atm of oxygen at the same temperature.

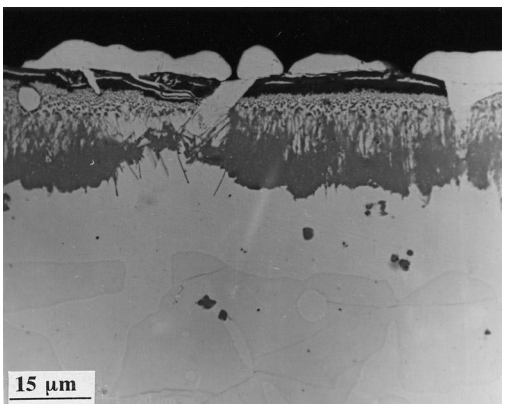


Fig. 4. Micrograph (SEM/BEI) of a cross section of Ag–8Y oxidized at 700°C under $10^{-20}$ atm $O_2$ for 24 h.

## 4. Discussion

The main differences between the scaling of Ag–8Y in 1 and $10^{-20}$ atm $O_2$ at 700°C are a large decrease of the corrosion rate and the formation of a continuous external $Y_2O_3$ layer under low P ($O_2$). Moreover, oxidation under low P ($O_2$) produces a layer of Y-depleted α phase beneath the ioz, while the io rate is largely decreased. The general scaling behavior of this alloy can be examined by means of a schematic isothermal phase diagram of the Ag-rich corner of the ternary Ag–Y–O system extending up to the β phase (the intermetallic compound $Ag_{51}Y_{14}$), shown in Fig. 5. The partial pressures of oxygen for the $Ag–Ag_2O$ and $\alpha–Ag_2O–Y_2O_3$ equilibria are denoted as $P_1$ and $P_2$, respectively, while $P_3$ corresponds to the $\alpha–\beta–Y_2O_3$ equilibrium and $P_1^g$, $P_2^g$ are the oxygen pressures in the gas phase used in the present work, equal to 1 and $10^{-20}$ atm $O_2$, respectively. The diffusion path corresponding to the behavior observed in 1 atm $O_2$ (dashed line) crosses the $\alpha+\beta$ two-phase field up to $P_3$ and then moves vertically upwards through the $\alpha+Y_2O_3$ field up to $P_1^g$, because no Y depletion occurs beneath the ioz in this case. On the contrary, the diffusion path for oxidation under $10^{-20}$ atm $O_2$ (dotted line) moves to the left up to the α phase line before reaching $P_3$, corresponding to the existence of a single-phase α layer beneath the ioz, and then moves into the $\alpha+Y_2O_3$ phase field up to an Y content equal to that of the original alloy at an oxygen pressure slightly above $P_3$, after which it moves vertically upwards for some distance, and finally moves completely to the $Y_2O_3$ corner (not shown in the figure) in correspondence to the continuous external layer of $Y_2O_3$. The possible reasons for the different scaling behavior of this alloy under the two different oxygen pressures are examined below.

An approximate calculation of the depth of internal oxidation in this alloy under 1 atm $O_2$ can be carried out as

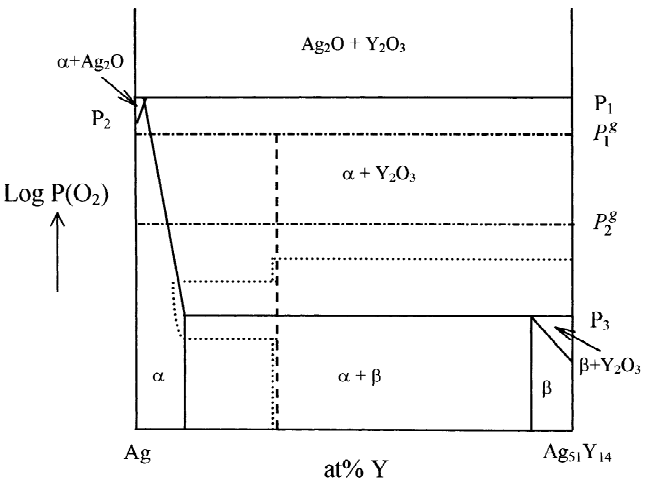


Fig. 5. Schematic isothermal phase diagram of the ternary Ag–Y–O system (Ag-rich corner) with the diffusion paths for oxidation under 1 atm $O_2$ (dashed line) and $10^{-20}$ atm $O_2$ (dotted line).

follows. The kinetics of internal oxidation of the most reactive component B in binary A–B alloys follow generally the parabolic rate law in the form [10–12]

$$\xi^2 = 4\gamma^2 D_0 t = k(\xi)t \quad (1)$$

where $\xi$ is the depth of internal oxidation, $t$ is time and $\gamma$ a kinetics parameter which, in the absence of external AO scales, is calculated from the basic equation given by Wagner [10–12]

$$N_O^s = \nu N_B^o G(\gamma)/F(h) \quad (2)$$

where $N_O^s$ is the solubility of oxygen in A, $N_B^o$ is the B content in the bulk alloy (mole fraction), $\nu$ the stoichiometric coefficient of oxygen in $BO_\nu$, $\gamma$ a dimensionless kinetics parameter and $h = \gamma\varphi^{1/2}$, with $\varphi = D_O/D_B$, while $D_O$, $D_B$ are the diffusion coefficients of O and B in A. Finally, $G(r)$ and $F(r)$ are two auxiliary functions defined as [11,12]

$$G(r) = \pi^{1/2} r \exp(r^2)\,\mathrm{erf}(r) \text{ and } F(r) = \pi^{1/2} r \exp(r^2)\,\mathrm{erfc}(r)$$

For the present case the diffusion of Y in the alloy is negligible: this corresponds to very small $D_B$ and very large $\varphi$ values, yielding $F(h) \cong 1$ [7,8]. Introduction of the values of the solubility (mole fraction) of oxygen under 1 atm $O_2$ [13] and of the diffusion coefficient of oxygen in Ag [13] in Eq. (2) yields $\gamma = 2.37 \times 10^{-2}$ and $k(\xi) = 2.79 \times 10^{-8}$ cm$^2$ s$^{-1}$. From this, the $\xi$ value calculated after 2 h is equal to 142 μm, and thus much larger than observed experimentally. The most likely reasons for this discrepancy are the presence of the internal oxide particles which hinder the inward flux of oxygen and that of the external layer of Ag, which can reduce the concentration of oxygen in Ag by decreasing the oxygen pressure at the external interface of the ioz with respect to that prevailing in the gas, according to Sievert's law [14]. In fact, in many cases of internal oxidation of two-phase binary alloys the actual internal oxidation depth was much larger than calculated by the approximations adopted here [15–21].

A similar calculation of $\xi$ cannot be made for the low P ($O_2$), because the $Y_2O_3$ layer on top of the alloy reduces the oxygen pressure at the alloy/scale interface below that prevailing in the gas phase by an unknown amount. The large reduction in the rate of internal oxidation is mostly due to the corresponding decrease in the concentration of oxygen dissolved in Ag. The simultaneous presence of the same oxide both as an external scale and as isolated particles in the alloy is very unusual in the oxidation of binary solid-solution alloys [22], but has been observed frequently in the oxidation of two-phase alloys [17,19,23–27].

The external oxidation of Y observed under low P ($O_2$) is rather surprising in view of its low content in the alloy and of the small solubility of Y in Ag (about 1 wt% at 700°C). In fact, a recent treatment of the internal oxidation of two-phase alloys [7,8] showed that the formation of external $BO_\nu$ scales on two-phase A–B alloys is only possible if a B-depleted layer of α phase, through which B can diffuse outwards sufficiently rapidly, forms above the bulk alloy. Even so, the critical B content for the transition from the internal to the external oxidation is significantly higher than for solid-solution alloys and increases quite rapidly when the solubility of B in the α phase decreases [7,8]. In particular, when the solubility of B is very small, the internal oxidation of B extends to quite high B contents and the process is entirely controlled by the penetration of the oxidant through the α-phase. In this condition, no significant outward diffusion of B can take place, leading to an in-situ or diffusionless internal oxidation [7,8]. Under these conditions, the spatial distribution of the oxide particles is expected to replicate quite closely that of the particles of the B-rich phase in the original alloy [6–8], as observed here for the oxidation under 1 atm $O_2$. On the contrary, during oxidation under low P ($O_2$) the inward diffusion of oxygen is considerably slowed down due to the presence of an external $Y_2O_3$ layer, so that Y can diffuse outwards through the alloy and the β phase dissolves beneath the io front: in this case, Y is sufficiently enriched in the external region of the ioz to produce a continuous $Y_2O_3$ layer on top of the alloy.

The change in the morphology of the internal particles of $Y_2O_3$ with the depth in the alloy is similar to what already reported for the nitridation of a Ni–10Cr–5Al alloy at 900°C [28]. There is no simple explanation available so far for this phenomenon, which depends on a complex interplay between the interface energy between the precipitate and the matrix and the strain energy due to precipitation [9,28,29]. On the contrary, the increase in the size of the globular particles in the external region of the ioz with depth in the alloy is in agreement with the theoretical prediction [9,28,29].

A final aspect concerns the presence of pure Ag in contact with the gas, as a continuous layer for the oxidation under 1 atm $O_2$ and as discontinuous particles under $10^{-20}$ atm $O_2$. An outward transport of the base metal through the ioz up to the alloy surface during the internal oxidation of binary alloys containing a noble component has already been reported for various systems [28]. In general, this produces nodules of the noble metal on the alloy surface [28], but in some special cases a continuous layer of metal has also been observed [16,18,30]. This process is due to the development of large compressive stresses in the ioz produced by the volume increase associated with the internal oxidation [28,31]. The solvent metal diffuses outwards to relieve these stresses by dislocation pipe diffusion, usually forming metal nodules over the alloy surface [28,31]. The formation of smaller amounts of Ag when oxidation is carried out under low P($O_2$) is a consequence of the existence of a continuous $Y_2O_3$ layer over the ioz, which, once completed, prevents the outward migration of Ag.

## 5. Conclusions

The oxidation of a two-phase Ag–8 wt% Y alloy at 700°C produces an internal oxidation of Y in a matrix of pure Ag. This is the only process occurring during oxidation in 1 atm $O_2$, while oxidation under $10^{-20}$ atm $O_2$ produces also a thin $Y_2O_3$ layer on top of the region of internal oxidation. At the same time, both the overall rate of oxidation and the rate of internal oxidation are significantly lower at low than at high oxygen pressures. Moreover, no significant diffusion of Y in the alloy occurs behind the front of internal oxidation during oxidation in 1 atm $O_2$, while oxidation under $10^{-20}$ atm $O_2$ produces a depletion of Y in the alloy and the formation of a layer of Y-depleted Ag-rich solid solution. The changes in both the kinetics and morphology of oxidation with the oxygen pressure in the gas are attributed to the reduced concentration and penetration of oxygen in the alloy under low P ($O_2$) as a consequence of the decrease of the oxygen pressure prevailing at the external alloy surface produced by the reduced pressure in the gas and by the presence of a surface layer of $Y_2O_3$. The formation of Ag nodules or even of a continuous Ag layer in contact with the alloy is due to a migration of Ag outwards induced by the large compressive stresses produced by the volume increase associated with the internal oxidation of Y.

## Acknowledgements

A financial support by the NNSF of China under the research projects (59725101-59871050) and by the Italian MURST through the National Research Project: ‘‘Leghe e Composti Intermetallici. Stabilità termodinamica, Proprietà Fisiche e Reattività’’ is gratefully acknowledged. Two of us (Y.N. and F.G.) are also grateful to CAS (China) and CNR (Italy) for a financial support for exchange visits through a collaboration agreement.

## References

[1] E. Lang (Ed.), The Role of Active Elements in the Oxidation Behavior of High Temperature Metals and Alloys, Elsevier Applied Science, London, 1989.
[2] F.H. Stott, G.C. Wood, J. Stringer, Oxid. Met. 44 (1995) 113.
[3] T. Massalski, Binary Alloys Phase Diagrams, ASM, Warrendale, USA, 1990.
[4] I. Barin, Thermodynamic Data for Pure Substances, VCH, Weinheim, Germany, 1989.
[5] F. Gesmundo, F. Viani, Y. Niu, Oxid. Met. 42 (1994) 409.
[6] F. Gesmundo, Y. Niu, F. Viani, Oxid. Met. 43 (1995) 379.
[7] F. Gesmundo, F. Viani, Y. Niu, Oxid. Met. 45 (1996) 51.
[8] F. Gesmundo, F. Viani, Y. Niu, Oxid. Met. 47 (1997) 355.
[9] F.H. Stott, G.C. Wood, Mater. Sci. Technol. 4 (1988) 1072.
[10] P. Kofstad, High Temperature Corrosion, Elsevier Applied Science, London, 1988.
[11] C. Wagner, Z. Elecktrochem. 63 (1959) 772.
[12] R.A. Rapp, Corrosion 21 (1965) 382.
[13] J.E. Verfurth, R.A. Rapp, Trans. Met. Soc. AIME 230 (1964) 1310.
[14] D.R. Gaskell, Introduction to the Thermodynamics of Materials, Taylor and Francis, Washington, 1995.
[15] F. Gesmundo, Y. Niu, F. Viani, F. Rizzo, Oxid. Met. 46 (1996) 441.
[16] W.T. Wu, R.Y. Yan, Y. Niu, F. Gesmundo, Corros. Sci. 39 (1997) 1831.
[17] Y. Niu, R.Y. Yan, G.Y. Fu, W.T. Wu, F. Gesmundo, Oxid. Met. 49 (1998) 91.
[18] G.Y. Fu, Y. Niu, W.T. Wu, F. Gesmundo, Corros. Sci. 40 (1998) 1215.
[19] Y. Niu, J.X. Song, F. Gesmundo, G.Y. Fu, C.L. Zeng, Corros. Sci. 42 (2000) 799.
[20] Y. Niu, Y.S. Li, F. Gesmundo, Corros. Sci. 42 (2000) 165.
[21] Y. Niu, Y.S. Li, F. Gesmundo, F. Viani, Intermetallics 8 (2000) 293.
[22] C. Wagner, Corros. Sci. 8 (1968) 889.
[23] Y. Niu, F. Gesmundo, F. Viani, W.T. Wu, Oxid. Met. 47 (1997) 21.
[24] Y. Niu, F. Gesmundo, D.L. Douglass, F. Viani, Oxid. Met. 48 (1997) 357.
[25] F. Gesmundo, Y. Niu, D. Oquab, C. Roos, B. Pieraggi, F. Viani, Oxid. Met. 49 (1998) 115.
[26] F. Gesmundo, Y. Niu, F. Viani, D.L. Douglass, Oxid. Met. 49 (1998) 147.
[27] Y. Niu, F. Gesmundo, G.Y. Fu, D.L. Douglass, Oxid. Met. 50 (1998) 327.
[28] D.L. Douglass, Oxid. Met. 44 (1995) 81.
[29] G. Bohm, M. Kahlweit, Acta Met. 12 (1964) 641.
[30] Z.L. Zhao, Y. Niu, F. Gesmundo, C.L. Wang, Oxid. Met. 54 (2000) 559.
[31] S. Guruswamy, S.M. Park, J.P. Hirth, R.A. Rapp, Oxid. Met. 26 (1986) 77.